Exploring the Importance of Sensors' Calibration in Inertial Navigation Systems

Konstantinos Papafotis
Department of Electrical and Computer Engineering
National Technical University of Athens, Greece
kpapafotis@mail.ntua.gr

Paul P. Sotiriadis
Department of Electrical and Computer Engineering
National Technical University of Athens, Greece
pps@ieee.org

***Abstract*—In this work, we explore the importance of sensors' calibration in inertial navigation applications. We focus on the case of low-cost systems, typically using MEMS inertial sensors, where the extra calibration cost is a critical parameter. We highlight the importance of calibration by deriving a bound of the evolution of the attitude and velocity error as a function of the calibration parameters' error. Then, we use low-cost 3-axis accelerometer and 3-axis gyroscope along with a popular pedestrian inertial navigation algorithm to experimentally confirm that raw sensor's data can be highly inappropriate for navigation purposes. Finally, we use the MAG.I.C.AL. methodology for joint calibration and axes alignment of inertial and magnetic sensors to achieve high accuracy measurements resulting in a reliable inertial navigation system.**

I. Introduction

Satellite-based systems (GPS, Galileo, GLONASS etc.) are the dominant navigation technology. Even though they provide sufficiently accurate navigation for most applications, they all come with the same drawbacks: they have limited refresh rate, they don't work in indoor environments and they are susceptible to jamming. To overcome these limitations, several alternative navigation technologies have been developed during the past decades. The concurrent development of the micro-electro-mechanical systems (MEMS) led to a significant growth of inertial navigation systems.

Inertial navigation systems (INS) are based on inertial sensors (accelerometers and gyroscopes) to calculate the velocity, orientation and position of a moving object. They are commonly used in a wide range of applications, from low-cost commercial systems, to high-end military, marine and aerospace applications. Although INS yield accurate short-term navigation, their long-term performance is degraded, mainly due to the heading error caused by gyroscope's noise and offset drift [1]. To improve the long-term performance, some authors combine INS with other navigation technologies (mostly satellite or RF based [2], [3]) while others use additional sensors (usually a magnetometer [1], [4]) to correct the estimated heading.

In the case of low-cost systems, MEMS inertial sensors are usually preferred due to their significantly lower cost and small size. However, a major disadvantage of MEMS inertial sensors is their large error characteristics [1]. Thus, in order to use them in an INS, a calibration procedure that compensates for the deterministic part of their error is required. In addition, the combined use of the accelerometer's, gyroscope's and maybe magnetometer's data gives rise to the need of alignment between the axes of the three sensors.

Although sensors' calibration and alignment are of major importance for an accurate INS, existing works take them for granted and only deal with the development of the navigation algorithms. Specifically, in [5], [6], [7], [8], [9], [10] expensive, already calibrated, commercially available sensor modules are used to evaluate the proposed algorithms. The authors in [2], [4], [11], [12] use custom sensor modules to evaluate the proposed INS but don't provide any details about the sensors' calibration and axes alignment.

Especially when low-cost systems are concerned, sensors' calibration and alignment could determine the overall system's cost. In the case of MEMS sensors, factory calibration is not an option as it would raise the sensors' cost significantly. In addition, standard after-production calibration and alignment techniques require expensive equipment (like a turn-table) that would also raise the overall system's cost.

In this work we derive the attitude and velocity error propagation equations as a function of accelerometer's and gyroscope's calibration parameters. Then, we design a low-cost inertial measurement unit (IMU) consisting of a MEMS 3-axis accelerometer and a MEMS 3-axis gyroscope. We calibrate the inertial sensors using the recently introduced MAG.I.C.AL. methodology [13] for joint calibration and axes alignment of inertial and magnetic sensors, and show how the raw sensors' data result in large attitude and velocity error. Finally, we use both the raw and calibrated sensors' data along with a popular pedestrian navigation algorithm, to experimentally demonstrate how the large error characteristics of the MEMS sensors affect the navigation accuracy.

II. Inertial Sensors' Error Characteristics and Measurement Model

There are several types of inertial sensors based on different operation principles and manufacturing technologies. Although the measurement accuracy varies extremely between different types, the basic error sources are the same for all inertial sensors.

- Bias, or offset, is a constant error exhibited by all inertial sensors. In most cases, it is the dominant term in the overall error of the sensor.

978-1-7281-3320-1/20/$31.00 ©2020 IEEE

- Scale-factor error is the deviation of the input-output gradient from unity.
- Cross-coupling error is caused by the non-orthogonality of the sensor's sensitivity axes due to manufacturing imperfections.
- Random noise is the non-deterministic error caused by both the mechanical and electronic structures of the sensors.

A widely accepted and highly referred measurement model for both 3-axis accelerometer and 3-axis gyroscope is the following [14] [1]

$$y = n + T_{sf}n + T_{cc}n + h + \varepsilon \tag{1}$$

where y is the 3×1 measurement vector, n is the 3×1 true specific force or angular velocity vector, T_{sf} is 3×3 matrix representing the scale-factor error, T_{cc} is 3×3 matrix representing the cross-coupling error, h is the 3×1 sensor's offset vector and ε is the 3×1 random error vector.

Most commonly, the compact form of (1) shown below is used

$$y = Tn + h + \varepsilon \tag{2}$$

where $T \triangleq I_3 + T_{sf} + T_{cc}$, and I_3 is the 3×3 identity matrix.

A calibration procedure compensates for the above errors by deriving the matrix T and offset vector h for which the error term in (2) is minimized.

III. Inertial Sensors' Error Propagation In The Inertial Frame

In this section the propagation of inertial sensors' error when they are used in navigation applications is described. In particular, we derive the error propagation equations in the inertial frame for attitude and velocity as a function of calibration parameters (T_a, h_a) and (T_g, h_g) of the accelerometer and gyroscope respectively.

A. Notation

Several different notations are used in the literature to describe kinematic quantities. In our analysis we will use the notation of [1]. More specifically, any kinematic quantity x, such as acceleration, velocity, position or angular velocity, is denoted as follows.

$$x^{\gamma}_{\beta\alpha}$$

where α is the body frame, β is the reference frame and γ is the resolving frame. In addition, the frame transformation matrix which transforms the resolving frame from α to β is denoted as C^{β}_{α}.

Also note that in the rest of this work, the true value of any quantity q is denoted as $\tilde{q}$ while the measured one is denoted as q.

B. Attitude Error Propagation

The attitude error in the inertial frame is defined as:

$$\delta C^i_b = \tilde{C^i_b} C^b_i \tag{3}$$

where $\tilde{C^i_b}$ is the true attitude while C^i_b is the attitude measured by the gyroscope. The differentiation of (3) yields

$$\delta \dot{C}^i_b = \dot{\tilde{C}}^i_b C^b_i + \tilde{C}^i_b \dot{C}^b_i \tag{4}$$

The time derivative of a coordinate transformation matrix is

$$\dot{C^{\beta}_{\alpha}} = C^{\beta}_{\alpha} \Omega^{\alpha}_{\beta\alpha} \tag{5}$$

where $\Omega^{\alpha}_{\beta\alpha}$ is the cross-product matrix of the angular velocity vector $\omega^{\alpha}_{\beta\alpha}$. Substituting the derivatives in (4), we get

$$\delta \dot{C}^i_b = \tilde{C}^i_b \, \delta\Omega \, \tilde{C}^b_i \, \delta C^i_b \tag{6}$$

where $\delta\Omega$ is the difference between the cross-product matrix of the true value of angular velocity vector $\tilde{\Omega^b_{ib}}$ and the one of the measured by the gyroscope angular velocity vector Ω^b_{ib}.

In our analysis we want to express $\delta \dot{C}^i_b$ as a function of the calibration parameters T_g and h_g. To that purpose, we express $\delta\Omega$ as a function of the gyroscope's measurement vector ω^b_{ib}:

$$\delta\Omega = \begin{bmatrix} P_1 \delta\omega & P_2 \delta\omega & P_3 \delta\omega \end{bmatrix} - \text{diag}(\delta\omega) \tag{7}$$

where $\delta\omega = (I_3 - T_g)\tilde{\omega} - h_g$, $P_1 = \begin{bmatrix} e_1 & e_3 & -e_2 \end{bmatrix}^T$, $P_2 = \begin{bmatrix} -e_3 & e_2 & e1 \end{bmatrix}^T$ and $P_3 = \begin{bmatrix} e_2 & -e_1 & e_3 \end{bmatrix}^T$. Note that e_k is the k^{th} normal vector in $\mathbb{R}^K$.

The evolution of the attitude error in time is

$$\delta C^i_b(t) = \int_0^t \delta \dot{C^i_b}(\tau) d\tau + \delta C^i_b(0) \tag{8}$$

Given that $\delta C^i_b(0) = I_3$ we write

$$\|\delta C^i_b(t) - I_3\| \leq \int_0^t \|\delta \dot{C^i_b}(\tau)\| d\tau \tag{9}$$

Taking the Frobenius norm of (6) we get

$$\|\delta \dot{C}^i_b\|_F \leq 15 \|\delta\omega\|_2 \tag{10}$$

Using (9) and (10), we write

$$\|\delta C^i_b(t) - I_3\| \leq 15t \left(\|I_3 - T_g\| w_B + \|h_g\| \right) \tag{11}$$

where w_B is a bound for the angular velocity magnitude and depends on the application.

C. Velocity Error Propagation

The velocity error is defined as

$$\delta V = \tilde{V} - V \tag{12}$$

The derivative of (12) is

$$\delta \dot{V} = \tilde{C}^i_b \tilde{f} - \delta C^i_b \tilde{C}^i_b \left(T_a \tilde{f} + h_a \right) \tag{13}$$

The evolution of the velocity error in time is derived by a similar analysis to that of the attitude error.

$$\delta V(t) \leq t \left[f_b \left(\|I_3 - T_a\| + \|T_a\| \|\delta C^i_b(t) - I_3\| \right) + \|h_a\| \right] \tag{14}$$

As seen in (14), the velocity error depends on both the accelerometer's and gyroscope's errors.

IV. Experimental Results

A. Pedestrian Inertial Navigation Using Shoe-Mounted Inertial Sensors

A common inertial navigation application is the pedestrian navigation with shoe-mounted inertial sensors. In this case, a 3-axis accelerometer and a 3-axis gyroscope are mounted on the shoe of a walking human. Using their data, the velocity, orientation and position are calculated.

In such applications, the zero velocity update (ZUPT) method is typically used [15] [8]. ZUPT method is based on the fact that during the stance phase of the human walking [9], the velocity of the shoe is zero. This information is usually used as input to a Kalman filter [15] [8] in order to correct the error of the velocity, orientation and position estimations.

In this work, we use the pedestrian navigation algorithm proposed in [15] to explore the effect of sensors' calibration on the navigation accuracy. The proposed algorithm in [15] provides accurate navigation using shoe-mounted inertial sensors and zero velocity updates in a Kalman filter architecture.

B. Experiment Procedure

Using a low-cost IMU, we recorded accelerometer's and gyroscope's measurements of a walking human. More specifically a $290m$ walk around the campus football court was recorded while the IMU was mounted on the shoe. In order to explore the importance of sensors' calibration, we reconstructed the walked trajectory using a) uncalibrated inertial sensors, b) calibrated accelerometer and offset compensated gyroscope and c) fully calibrated accelerometer and gyroscope.

For the inertial sensors' calibration, we exploited the recently introduced MAG.I.C.AL. methodology. MAG.I.C.AL. provides unified calibration and joint axes alignment of 3-axis magnetometer, 3-axis accelerometer and 3-axis gyroscope. MAG.I.C.AL. compensates for all linear time-invariant distortions such as scale-factor, cross-coupling and offset, including the soft-iron and hard-iron distortion of the magnetometer. It is applied in a simple 15-step sequence of approximate placements and rotations of the sensors, made by hand, without requiring any special piece of equipment.

C. Error Propagation

In Section III a bound for the evolution of attitude error as a function of accelerometer's and gyroscope's calibration parameters is derived. Using the calibration parameters calculated using MAG.I.C.AL. methodology and the analysis of Section III we can explore the effect of calibration on the attitude and velocity error propagation.

In Figure 1 the evolution of attitude error in time is presented. As seen in Figure 1 the attitude error rises significantly after a few seconds when using uncalibrated sensors. Accelerometer's calibration and gyroscopes offset compensation improves the error evolution significantly but eventually large attitude errors are accumulated.

In Figure 2 the evolution of velocity error in time is shown. As in the case of attitude, the velocity error also rises significantly after a few seconds when using uncalibrated sensors. Also note that, according to Figure 2, the gyroscope's error is the dominant error factor in the velocity error.

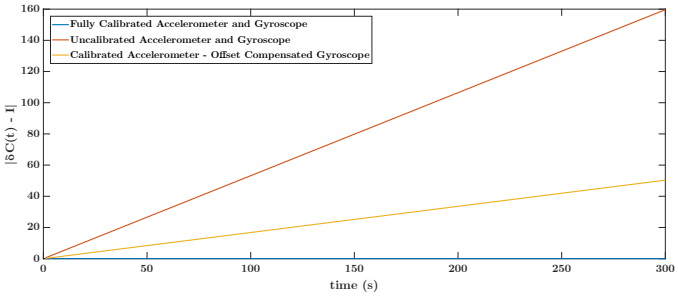

Fig. 1: Evolution of attitude error in time.

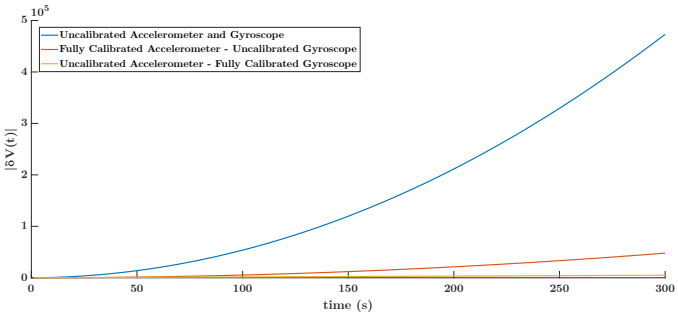

Fig. 2: Evolution of velocity error in time.

D. Trajectory reconstruction

The reconstructed trajectory using raw sensor's data is depicted in Figure 3a. As seen in Figure 3a, raw sensor's data are highly inappropriate for navigation purposes.

For accelerometer's calibration, there are several easy-to-apply methods without requiring any special piece of equipment [16], [13], [17]. In addition, although gyroscope's calibration is not trivial without using appropriate equipment, it's offset is easy to remove as it is just the sensor's output while it is still. By doing so, the navigation results are significantly improved as shown in Figure 3b.

In Figure 3c the reconstructed trajectory using calibrated inertial sensors is presented. The trajectory shown in Figure 3c, exhibit a position error of about 5m in a 290m walk. The resulted navigation performance may not be state-of-the-art but it is actually impressive considering that we used very low-cost sensors and no special calibration equipment. In addition, the navigation algorithm used in this work is a basic algorithm using only inertial sensors. More complicated algorithms as well as the use of extra sensors (such as magnetometer) would provide even smaller position error.

Note that as seen in both Figures 3b and 3c the GPS sampling rate is quite low causing sharp corners in the reconstructed trajectory.

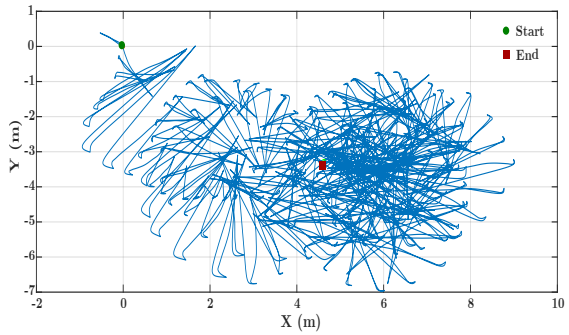

(a)

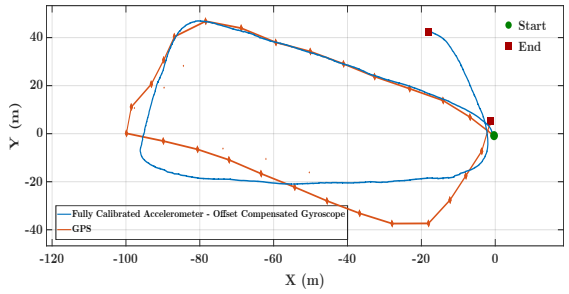

(b)

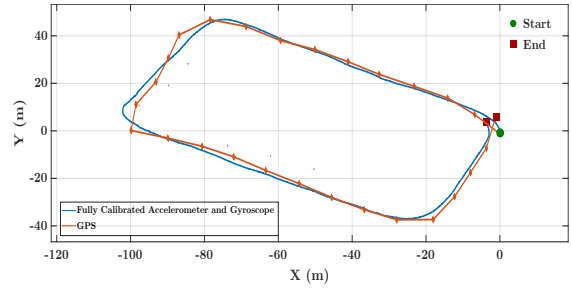

(c)

Fig. 3: Reconstructed trajectory using a) uncalibrated inertial sensors, b) calibrated accelerometer and offset compensated gyroscope and c) fully calibrated inertial sensors

V. Conclusion

In this work we highlighted the importance of the inertial sensors' calibration when they are used in navigation applications. We derived a mathematical model for the evolution of the attitude and velocity errors as a function of the inertial sensors' calibration parameters. Using it we demonstrated how using uncalibrated sensors, large errors in attitude and velocity are accumulated over time. Then we used MAG.I.C.AL. methodology for joint calibration and axes alignment of the inertial sensors to compensate for the aforementioned errors. Finally we used a popular pedestrian navigation algorithm to experimentally demonstrate the effect of the sensors' errors in the navigation procedure. Both mathematical analysis and experimental results indicate that inertial sensors' calibration is of critical importance when they are used in navigation applications.

Acknowledgment

This research is co-financed by Greece and the European Union (European Social Fund- ESF) through the Operational Programme "Human Resources Development, Education and Lifelong Learning" in the context of the project "Strengthening Human Resources Research Potential via Doctorate Research" (MIS-5000432), implemented by the State Scholarships Foundation (IKY).

The authors acknowledge financial support from Weasic Microelectronics S.A. for partial covering of the conference attendance expenses.

References

[1] P. D. Groves, *Principles of GNSS, Inertial, and Multisensor Integrated Navigation Systems*. Artech House, 2013.

[2] J.-O. Nilsson, D. Zachariah, I. Skog, and P. Händel, "Cooperative localization by dual foot-mounted inertial sensors and inter-agent ranging," *EURASIP Journal on Advances in Signal Processing*, vol. 2013, no. 1, p. 164, Oct 2013. [Online]. Available: https://doi.org/10.1186/1687-6180-2013-164

[3] R. Jirawimut, P. Ptasinski, V. Garaj, F. Cecelja, and W. Balachandran, "A method for dead reckoning parameter correction in pedestrian navigation system," in *IMTC 2001. Proceedings of the 18th IEEE Instrumentation and Measurement Technology Conference. Rediscovering Measurement in the Age of Informatics (Cat. No.01CH 37188)*, vol. 3, May 2001, pp. 1554–1558 vol.3.

[4] R. Stirling, J. Collin, K. Fyfe, and G. Lachapelle, "An innovative shoe-mounted pedestrian navigation system," 01 2003, pp. 110–5.

[5] H. Guo, M. Uradzinski, H. Yin, and M. Yu, "Indoor positioning based on foot-mounted imu," *Bulletin of the Polish Academy of Sciences Technical Sciences*, vol. 63, 09 2015.

[6] A. R. Jimenez, F. Seco, C. Prieto, and J. Guevara, "A comparison of pedestrian dead-reckoning algorithms using a low-cost mems imu," in *2009 IEEE International Symposium on Intelligent Signal Processing*, Aug 2009, pp. 37–42.

[7] A. R. Jiménez, F. Seco, J. C. Prieto, and J. Guevara, "Indoor pedestrian navigation using an ins/ekf framework for yaw drift reduction and a foot-mounted imu," in *2010 7th Workshop on Positioning, Navigation and Communication*, March 2010, pp. 135–143.

[8] E. Foxlin, "Pedestrian tracking with shoe-mounted inertial sensors," *IEEE Computer Graphics and Applications*, vol. 25, no. 6, pp. 38–46, Nov 2005.

[9] O. Bebek, M. A. Suster, S. Rajgopal, M. J. Fu, X. Huang, M. C. Cavusoglu, D. J. Young, M. Mehregany, A. J. van den Bogert, and C. H. Mastrangelo, "Personal navigation via high-resolution gait-corrected inertial measurement units," *IEEE Transactions on Instrumentation and Measurement*, vol. 59, no. 11, pp. 3018–3027, Nov 2010.

[10] R. Feliz, E. Zalama, and J. Gómez-García-Bermejo, "Pedestrian tracking using inertial sensors," *Journal of Physical Agents*, vol. 3, 01 2009.

[11] S. Yun Cho and C. Gook Park, "Mems based pedestrian navigation system," *Journal of Navigation*, vol. 59, pp. 135 – 153, 01 2006.

[12] J. Nilsson, A. K. Gupta, and P. Händel, "Foot-mounted inertial navigation made easy," in *2014 International Conference on Indoor Positioning and Indoor Navigation (IPIN)*, Oct 2014, pp. 24–29.

[13] K. Papafotis and P. P. Sotiriadis, "Mag.i.c.al.–a unified methodology for magnetic and inertial sensors calibration and alignment," *IEEE Sensors Journal*, vol. 19, no. 18, pp. 8241–8251, Sep. 2019.

[14] A. Noureldin, T. B. Karamat, and J. Georgy, *Fundamentals of Inertial Navigation, Satellite-based Positioning and their Integration*. Springer-Verlag Berlin Heidelberg, 2013.

[15] C. Fischer, P. Talkad Sukumar, and M. Hazas, "Tutorial: Implementing a pedestrian tracker using inertial sensors," *IEEE Pervasive Computing*, vol. 12, no. 2, pp. 17–27, April 2013.

[16] N. Ammann, A. Derksen, and C. Heck, "A novel magnetometer-accelerometer calibration based on a least squares approach," in *2015 International Conference on Unmanned Aircraft Systems (ICUAS)*, June 2015, pp. 577–585.

[17] Y. Zhong, Y. Xu, N. He, and X. Yu, "A new drone accelerometer calibration method," in *2018 37th Chinese Control Conference (CCC)*, July 2018, pp. 9928–9933.